NASA TN D-23

TECHNICAL NOTE
D-23

EXPERIMENTAL OPERATING PERFORMANCE OF A SINGLE-STAGE ANNULAR AIR EJECTOR

By Robert R. Howell

Langley Research Center
Langley Field, Va.

NATIONAL AERONAUTICS AND SPACE ADMINISTRATION

WASHINGTON

October 1959

NATIONAL AERONAUTICS AND SPACE ADMINISTRATION

TECHNICAL NOTE D-23

EXPERIMENTAL OPERATING PERFORMANCE OF A SINGLE-STAGE ANNULAR AIR EJECTOR

By Robert R. Howell

SUMMARY

The experimental performance of a small-scale single-stage annular air ejector has been established for a range of pressures and weight flows which allow the ejector to be used as a pump on the discharge end of a hypersonic blowdown wind tunnel. A limited study was also made of the starting-pressure requirements for two conical-nozzle test-section arrangements and of the effect of the presence of bluff bodies on the flow in a free-jet test section.

The results of the investigation indicated that such an ejector could be designed to evacuate statically to a pressure of at least 0.03 atmosphere. One-dimensional theory predicts satisfactorily the maximum static-pumping ability of the ejector. The minimum pressure for which it could be designed to evacuate while pumping weight flow was indicated to be primarily a function of the Mach number established in the mixing tube and the ratio of weight flow through the ejector to the weight flow being pumped. The effect of this weight-flow ratio became increasingly important as the ratio was reduced to 15 or less. It was concluded that a single-stage annular air ejector could be designed to produce a pumping pressure as low as about 0.06 atmosphere provided sufficient storage volume, pressure, and weight flow were available to establish the correct Mach number in the mixing tube and the correct ratio of ejector weight flow to pumped weight flow.

The limited study of hypersonic test-section arrangements indicated that it was desirable to use a supersonic diffuser downstream of the test section. For the open test section a diffuser having a contraction ratio of roughly 0.6 appeared to be optimum. Tests of blunt bodies in an open test section indicated that the size for testing would have to be limited to body sizes considerably smaller than would be estimated on the basis of one-dimensional blockage.

INTRODUCTION

High-performance air ejectors are of interest as a possible means by which the discharge pressure of hypersonic wind tunnels can be reduced; this reduction would permit wind-tunnel operation at low stagnation pressures.

The air-ejector type of pump utilizes the pressure drop associated with a jet having a large weight flow and high velocity to aspirate or pump gas from a low pressure to a higher one. General studies of ejectors, both analytical and experimental, are numerable. (See, e.g., refs. 1 to 4.) There are also some data available to indicate the performance of small low-density wind tunnels which utilize air or steam ejectors. (See, e.g., refs. 5 and 6.) However, experimentally determined performances of ejector designs suitable for use with hypersonic wind tunnels are essentially nonexistent.

This paper presents some of the experimentally determined performance characteristics of a single-stage annular air ejector operating in the ranges of pressure and weight-flow ratios which are required when the ejector is used with a hypersonic wind tunnel. Where possible, the experimental results are compared with results obtained using one-dimensional theory. Also presented are limited data showing (1) starting-pressure requirements for some conical-nozzle—test-section arrangements which discharged to the ejector and (2) the effect of the presence of bluff bodies on the flow in a free-jet test section.

SYMBOLS

A	area, sq in.
D	diameter
M	Mach number
p	static pressure, psi
p_a	atmospheric pressure (taken as 14.7 psi)
p_t	total pressure, psi
r	ratio of airflow through ejector to airflow through conical nozzle

x,y rectangular coordinates

Subscripts:

b body

c plenum chamber

e exit conditions for nozzles flowing full with supersonic flow

j ejector

l lower nozzle

m mixing tube

n nozzle

u upper nozzle

2 condition at second minimum

Superscripts:

* sonic conditions or minimum area

' behind normal shock

APPARATUS

Two ejector—mixing-tube combinations were tested. The first configuration consisted of an annular air ejector discharging into a straight mixing tube (fig. 1). The ejector-nozzle contours (table I) were scaled from ones calculated for a two-dimensional adjustable nozzle. (See ref. 7.) The use of a two-dimensional contour for the design of the ejector nozzle appeared justified inasmuch as the diameter of the annular exit was large compared to the annular width. The inner nozzle contour could be translated relative to the fixed outer contour by means of the screw threads shown in figure 1. In this manner the Mach number developed at the ejector-nozzle exit could be changed. High-pressure air was introduced to the annular ejector plenum chamber from a 2-inch-diameter supply ring through eight 1/2-inch-diameter distribution tubes. From the plenum chamber the air expanded through the ejector nozzle into the mixing tube and thence to the atmosphere through the subsonic diffuser. This ejector configuration as shown in figure 1 will be denoted hereafter as ejector 1.

The second ejector configuration, which will be denoted as ejector 2, differed from ejector 1 only in mixing-tube geometry. For this design the inside diameter of the mixing tube was increased as shown in figure 2, and a contraction or second minimum was incorporated at its downstream end.

Airflow to be pumped by the ejector was in every case introduced through a conical nozzle having sufficient area expansion to develop hypersonic velocity if a sufficient pressure ratio were applied across it. With ejector 1 the conical nozzle was tested with a closed test section (fig. 3). With ejector 2 the conical nozzle used varied in geometry (fig. 4) and was tested with an open test section as shown in figure 5. In this test-section arrangement the conical nozzle could be shifted longitudinally to vary the length of the open test section and the downstream supersonic diffuser could be changed. Windows on either side of the test-section chamber allowed visualization of the open jet through the use of a schlieren system.

A sketch of the overall arrangement of the apparatus is shown in figure 6 and a photograph of it is shown in figure 7. The large plenum chamber shown between the test section and the ejector was introduced in order that nozzle discharge pressure could be measured independently of velocity effects. The pressure measured in the plenum chamber was used to determine the pressure ratio across the nozzle—test-section arrangement or to determine the pressure to which the ejector could evacuate while pumping varying weight flows.

TESTS

For tests the stagnation pressure to the ejector and conical nozzle was controlled manually by adjusting valves to maintain the desired pressure. The stagnation pressures were indicated on 16-inch Bourdon type pressure gages. These gages were calibrated and found to be accurate to within ±1.0 psi. Static pressures in the mixing tube and in the exit of the ejector nozzle, as well as in the test-section chamber and plenum chamber, were obtained from the deflection of the mercury column in a multitube manometer. The pressures so measured are believed to be correct to within ±0.1 psi. All pressures were recorded simultaneously by photographing together the manometer board and dial gages with a single camera. The pressure in the plenum chamber was also recorded from visual reading of the deflection of a precision mercury column. Such readings are believed to be accurate to within ±0.01 psi.

Air for the tests was obtained from a system providing dry air at pressures up to 500 psia and at total temperatures between 70° and 150° F. No heater was used to boost this temperature, and, therefore, some

liquefaction of air must have occurred in the test sections and in the ejector mixing tube where relatively high Mach numbers were encountered. Reference 8, however, indicates that the effect of this possible liquefaction on measured nozzle pitot-pressure ratios, and consequently, on nozzle starting-pressure ratios, should be negligible.

The Mach number at the ejector exit, which did not exceed about 3.4, was calibrated as a function of longitudinal displacement of the inner nozzle contour. The calibration was made using the ratio of the static pressure in the nozzle exit to the stagnation pressure as an indication of Mach number. The longitudinal displacement was indicated on a precision dial indicator accurate to ±0.001 inch. The calibration is presented in figure 8. Also shown in the figure are the two design points used in deriving the theoretical nozzle contour. Repeated checks on the calibration showed that the displacement measurement indicated the Mach number at the ejector exit correctly to within ±0.03. This was considered to be sufficiently accurate for the purpose of repeating nozzle settings for these experiments.

RESULTS AND DISCUSSION

Static-Pumping Characteristics

The experimental pumping characteristics of the ejector designs for the case in which no weight flow is pumped are presented as figures 9(a) and 9(b) for various Mach numbers at the ejector nozzle exit. The pressure in the large plenum chamber $\frac{p_c}{p_a}$ produced by the ejector is presented as a function of the stagnation pressure $\frac{p_{t,j}}{p_a}$ applied to the ejector for the various nozzle settings. For both designs, increasing the Mach number at the ejector exit resulted in a decrease in the minimum value of $\frac{p_c}{p_a}$ produced. This minimum, however, occurred in every case at a higher stagnation pressure. This trend is explained by the fact that the pressure in the plenum chamber for this no-flow case must be in equilibrium with the static pressure in the upstream end of the mixing tube. The minimum pressure at this point in the tube occurs when the tube first flows full with supersonic flow. The supersonic Mach number at this point is dependent upon the ratio of mixing-tube cross-sectional area to the minimum or throat area of the ejector nozzle $\frac{A_m}{A_j^*}$ and is established by applying a required starting pressure ratio across the ejector system.

The throat area of the ejector for the present case varies with the nozzle setting so that it decreases as the Mach number at the ejector exit increases. Hence, as the ejector-exit Mach number is increased, the area ratio $\frac{A_m}{A_j^*}$ is increased, thereby developing a higher supersonic Mach number in the mixing tube and requiring a correspondingly higher starting pressure.

A comparison of the minimum pressure produced by the ejector as a function of the area ratio $\frac{A_m}{A_j^*}$ is presented in figure 10. The test-point symbols used correspond to the ejector settings of figures 9(a) and 9(b) for ejector 1 and ejector 2, respectively. Also shown is the pressure that can be developed theoretically by one-dimensional expansion of the ejector airflow through the area ratio $\frac{A_m}{A_j^*}$ if a normal shock loss is assumed to determine the starting pressure $\frac{p_{t,j}}{p_a}$. The pumping ability of ejector 2 appears to agree very well with what would be expected on the basis of the one-dimensional calculations. Ejector 1 does not agree so well quantitatively, although the apparent trend is correct. The small $\left(\Delta \frac{p_c}{p_a} \approx 0.02\right)$ apparent difference in pumping ability indicated for the two designs is believed to be associated primarily with the differences in weight flow for the two cases. Approximately twice as much weight flow was required for optimum pumping with ejector 2 as was required for ejector 1 for the same value of $\frac{A_m}{A_j^*}$. This, of course, results from the increase in mixing-tube cross-sectional area A_m for ejector 2 design. It is believed that the mixing losses at the free boundary of the flow from the annular ejector nozzle are essentially constant for the case of equilibrium pumping. Hence, for a particular value of $\frac{A_m}{A_j^*}$, the mean momentum, and therefore pumping ability, of the ejector is increased as the total mass flow through the ejector is increased by increasing A_m. The differences in internal geometry of the two mixing tubes should not affect large changes in pumping ability.

The test results as compared with theory indicate that further increases in values of $\frac{A_m}{A_j^*}$ beyond those values tested would not result in further significant decreases in minimum static-pumping pressure.

The stagnation pressure required to establish supersonic flow in the mixing tube or to achieve minimum pressure is presented for the two designs as a function of $\frac{A_m}{A_j^*}$ in figure 11. Also presented is the one-dimensional starting pressure required which is calculated by assuming normal shock losses. There appears to be no difference in the starting-pressure requirement of the two designs, as indicated by the overlap of data points. It is apparent that, for starting, losses somewhat greater than those for normal shock (as much as 20 percent greater) generally existed in the small-scale apparatus for the starting-pressure range less than $\frac{p_{t,j}}{p_a} \approx 22$. At the maximum pressure of the present tests, agreement with the theory was indicated. It should be noted that as a result of the required increase in $\frac{p_{t,j}}{p_a}$ with increasing area ratios $\frac{A_m}{A_j^*}$, the weight flow necessary to produce a given pressure (greater than the minimum) is essentially constant for a given design and is fixed primarily by the value of A_m. It should also be noted that as a result of the contraction or second minimum incorporated in the design of ejector 2, a hysteresis loop could be obtained in the pressure curve as indicated by the typical curve shown in figure 12. For this design the second minimum allows the mixing-tube flow, once it becomes supersonic, to remain supersonic at stagnation pressures lower than the stagnation pressure required for starting. Hence, minimum pressures slightly lower than those indicated for the configuration (fig. 10) could be obtained by starting the mixing tube at supersonic speeds and then reducing the stagnation pressure. The actual amount that the pressure can be reduced and still maintain supersonic flow is a function of the ratio of second-minimum area to mixing-tube area. For the present case the ratio was 0.70 and the pressure could be reduced approximately 10 percent for the no-flow case.

The static-pumping results indicate that a single-stage annular air ejector can be designed to evacuate to a static pressure of at least 0.03 atmosphere, dependent upon the stagnation pressure that is available to the ejector. It is also shown that one-dimensional theory gives a good indication of the possible minimum pressure to be expected for any particular value of $\frac{A_m}{A_j^*}$.

Pumping Characteristics With Flow

Typical pumping characteristics of ejector 2 are presented as figure 13 for ratios of mixing-tube area to ejector-throat area of 23.65, 17.21, and 14.31. Presented is the pressure to which the ejector will evacuate while pumping varying amounts of flow at varying ejector stagnation pressures. Also shown is the pressure to which the ejector would evacuate while pumping no flow. This, of course, corresponds to a mass ratio of $r = \infty$. It is shown that at ejector stagnation pressures lower than that required for starting the mixing tube, variation in mass ratio r has little effect on the pressure produced. Once the flow in the mixing tube is started (the started condition corresponds to the bottom curve in the figure), however, decreases in mass ratio (corresponds to increasing the weight flow pumped) result in significant increases in the evacuation pressure $\frac{p_c}{p_a}$, especially at values of r less than about 15. (See, e.g., fig. 13(b).)

L
4
3
8

No attempt was made to compare these experimental results with theory inasmuch as no measurements of the losses through the nozzle—test-section arrangement were obtained. Apparently, the losses were about constant for all arrangements tested and under all conditions, as indicated by the overlap of the data from the various nozzle configurations. For example, in figure 13(b), for $p_{t,j} = 13.23$ atmospheres, the $\frac{A}{A^*} = 247$ nozzle was started at $r = 55$. The $\frac{A}{A^*} = 97.2$ nozzle did not start until $r = 21$. Therefore, near $r = 50$ the flow in the $M_{n,e} \approx 8.4$ nozzle was flowing full and hypersonic, whereas the flow in the $M_{n,e} \approx 6.8$ nozzle was only slightly supersonic near its throat. The ejector pumped to about the same pressure for both cases indicating that the overall losses for both nozzles are about the same although they were operating under greatly different conditions.

The data for the $\frac{A}{A^*} = 117$ nozzle and the $\frac{A}{A^*} = 247$ nozzle for $p_{t,j} = 12.5$ atmospheres (fig. 13(b)) were obtained on the low-pressure side of the hysteresis loop discussed previously, thereby explaining the lower pressures produced at the lower ejection stagnation pressure.

By comparing the pumping characteristics of the ejector at three area-ratio settings $\frac{A_m}{A_j^*}$ (fig. 13), the effect of $\frac{A_m}{A_j^*}$ is discerned.

Generally, as the area ratio is increased at constant mass ratio r a higher ejector stagnation pressure $p_{t,j}$ is required to achieve a given evacuation pressure and the minimum pressure producible is lowered. This trend, of course, is similar to that obtained in the static-pumping case where no flow was pumped. Generally, it is indicated that a single-stage annular air ejector can be designed to produce pumping pressure of, at least, about 0.06 atmosphere provided that $\frac{A_m}{A_j^*}$ is large enough and that the available pressure and weight flow are sufficient to give the desired value of weight-flow ratio. If it is desired to produce a pumping pressure of less than 0.2 atmosphere obviously weight-flow ratios greater than 10 should be employed. It should be noted that when ejectors are used in conjunction with a hypersonic nozzle, large values of r do not necessarily indicate extreme ejector flow rates. The weight flow per unit of test-section area is relatively small for hypersonic nozzles as compared with, say, the weight flow for an M = 2.0 nozzle; therefore, a hypersonic-nozzle—ejector combination of acceptable scale can be operated with the same flow rate that would normally pass through a usable M = 2.0 nozzle alone. (This is assuming that adequate pressure is available.)

It should be pointed out that the present experiments do not include the effect of differences in stagnation temperature between the ejector flow and the flow being pumped. For example, if the ejector is using cold air and is pumping hot air the mass ratio required to achieve a specified pumping pressure would be greater than that required for the present case where the temperatures of both flows are the same. No experimental study showing this effect of differences in temperatures on ejector performance has been found in the literature. An indication of it may be obtained, however, from calculations following a method such as that proposed in reference 5.

Wall pressure distributions along the mixing tube for ejector 2 are presented in figure 14 for the case of the started mixing tube. These pressures are presented primarily to show the pressure loads that might be experienced by the tube shell under maximum pumping conditions. Relatively small changes in local pressure are indicated for the range of mass ratio shown. This would probably be expected inasmuch as the mass-ratio range presented is the end of the range where the evacuation pressure produced by the ejector changes only slightly with relatively large changes in mass ratio. At the upstream end of the tube fair agreement with the calculated pressure is indicated. The pressure indicated for the larger area ratio is somewhat higher than the calculated pressure which may be a result of the presence of air liquefaction.

Effect of Variation in Wind-Tunnel Geometry

Inasmuch as data obtained at the present scale and in the presence of possible air liquefaction do not provide a sound basis for the design of a large-scale high-temperature wind tunnel, only limited experimenting with wind-tunnel geometry was made. Of these limited data only those believed to be of general interest are presented, namely, (1) starting-pressure requirements for the $M \approx 6.8$ nozzle with varying ejector settings, (2) variation of starting-pressure requirements for various second-minimum contraction ratios for the open test section, and (3) effect of model size on the open-jet flow characteristics.

Closed test section.- Pressures required to start the combination of the $M_{n,e} \approx 6.8$ nozzle and the closed test section (fig. 3) as a function of $\frac{A_m}{A_j^*}$ (ejector 1) are presented in figure 15. The starting pressure for this case was determined as the nozzle stagnation pressure required for the ratio of pitot pressures to nozzle stagnation pressures to become a constant value. This starting pressure was easily discerned inasmuch as the pitot pressure approached a constant presentage of $p_{t,n}$ almost discontinuously as the nozzle started. The results presented in figure 15 clearly indicate the advantage of using as large a ratio of mixing-tube area to nozzle-throat area as possible when designing the ejector. It is also indicated to be highly desirable to use a second minimum between the test section and ejector rather than a long straight tube. The scatter of data points for the case with a second minimum results from a small variation in weight-flow ratio r. The overall range of r encompassed by the data shown is from $r = 9.7$ to $r = 12.5$. The corresponding range of ejector stagnation pressure is from $p_{t,j} = 14.9$ to $p_{t,j} = 17.5$ atmospheres. The flagged symbols presented in figure 15 were calculated (ref. 5) by using experimental pressures and the actual geometric areas of the apparatus. These points indicate that the experimental starting pressure was as much as 40 percent higher than the theoretical starting pressure for tests both with and without the supersonic diffuser. This difference between the theoretical and experimental pressures is larger than is generally experienced and is believed to be associated with the large second minimum $\frac{A_2^*}{A_{n,e}} = 0.714$. Unpublished data obtained at other facilities indicate that, if a more-optimum area ratio, say, $\frac{A_2^*}{A_n} = 0.6$, had been tried, this difference between theory and experiment would have been considerably reduced.

The $M_{n,e} \approx 6.8$ nozzle test section could be started with a stagnation pressure at least as low as 9 atmospheres. The ejector for this case required a stagnation pressure of about 17 atmospheres indicating that hypersonic facilities can be started and operated with air from a low-pressure storage without the use of a vacuum tank provided that sufficient air-storage volume and weight flow are available to allow the use of an air ejector for the purpose of reducing the tunnel discharge pressure.

Open test section.- The open- or free-jet test section is of considerable interest for use with high-temperature jets in that it alleviates by virtue of the essentially unlimited space around the jet the need for large window openings in the test-section wall for model and flow visualization. Such a design also eliminates the need for doors that must open, close, and seal when models are placed in and removed from the jet. During the present investigation the following two characteristics of open test sections were studied briefly: (1) the variation of nozzle starting stagnation pressure with the second-minimum contraction ratio $\frac{A_2^*}{A_{n,e}}$ and (2) the effect of blunt model size on the test-section flow characteristics.

For the case of the open test section (fig. 5) the starting pressure was designated as that pressure required to cause the boundary of the free jet to be at least parallel to the axis (no model in the jet) and was determined by watching a schlieren picture of the jet flow and varying the nozzle stagnation pressure. Figure 16 presents the starting and minimum operating pressure thus determined as a function of the second-minimum contraction ratio for two conical nozzles and for ejector 2 operating at a fixed condition. The $M_{n,e} \approx 7.1$ nozzle could be started at pressures as low as 9 atmospheres with the ejector operating at 13.23 atmospheres. The $M_{n,e} \approx 8.4$ nozzle could similarly be started with 16 to 18 atmospheres of pressure. A comparison between the starting pressures for this open test section and those for the previously discussed closed test section cannot be made directly because of the difference in nozzle dimensions and weight flow through the two ejector designs. For the open test section with an $M_{n,e} \approx 7.1$ nozzle, the value of r at starting was about 30 which was roughly three times the value of r required for starting the closed test section $\left(M_{n,e} \approx 6.8 \text{ nozzle combination}\right)$. From this fact it is apparent that the starting-pressure requirements for the open test section would be somewhat higher than those for the closed test section if the two arrangements were checked with the same ejector pumping conditions.

A contraction ratio $\frac{A_2^*}{A_{n,e}}$ of about 0.6 is indicated to be near optimum for the two cases presented. This value of contraction ratio agrees well with the one-dimensional starting area ratio calculated (assuming normal shock losses). It should be noted that the minimum operating pressure is considerably lower than the starting pressure for contraction ratios near the apparent optimum. (Operating pressure is approximately 3 atmospheres lower than starting pressure for the $M_{n,e} \approx 7.1$ nozzle and approximately 8 atmospheres lower for the $M_{n,e} \approx 8.4$ nozzle.)

One of the possible disadvantages of the open test section is that it cannot tolerate losses such as those experienced when bluff bodies are introduced into the flow. The equilibrium pressure established in the chamber surrounding the jet is dependent upon the aspirating ability of the jet itself. The loss in average momentum of the jet across the test section resulting from the presence of a bluff body therefore shows up directly as an increase in chamber pressure and a consequent convergence of the jet boundary. This effect is clearly demonstrated in figure 17 which shows the increase in the convergence angle of the jet boundary as the bluff-body size has increased. In all cases the jet flow was established without the body present and then the body was inserted into the jet flow. The pictures for $\frac{D_b}{D_{n,e}} = 0.286$ (fig. 17(c)) show the jet-flow breakdown as a body which was too large for the jet was lowered into it. The jet boundary for this case converged with increasing angle as the body was lowered until, as the body approached the center line, all traces of supersonic flow disappeared. It should be noted that the body frontal area here is only about 8 percent of the nozzle exit area and, hence, much smaller than the allowable blockage based on calculation using one-dimensional theory.

Increasing nozzle stagnation pressure reduced the convergence angle of the jet boundary as is shown in figures 17(a) and (b). This effect most probably is a result of the increased mass flow through the nozzle with increased stagnation pressure which, of course, aids the jet in aspirating. It should again be pointed out that when examining these data or comparing them with other data allowances should be made for the possible effects of air liquefaction and model scale.

CONCLUDING REMARKS

The experimental performance of a single-stage annular air ejector has been established for a range of stagnation pressures and weight flows

which allows the ejector to be used as a pump on the discharge end of a hypersonic blowdown wind tunnel. A limited study was also made of the starting-pressure requirements for two conical-nozzle test-section arrangements and of the effect of the presence of bluff bodies on the flow in a free-jet test section.

The results of the investigation indicated that annular air ejectors could be designed to evacuate to at least 0.03 atmosphere while pumping statically. One-dimensional theory predicts satisfactorily the maximum static-pumping ability of the ejector. The minimum pressure such a design would produce while pumping flow was indicated to be a function of the Mach number produced in the mixing tube and the ratio of the weight flow passed through the ejector to the weight flow being pumped. The effect of this weight-flow ratio became increasingly important as the ratio approached 15 or less.

It was concluded that a single-stage annular air ejector could be designed to provide a pumping pressure as low as about 0.06 atmosphere provided that sufficient storage pressure, volume, and weight flow are available to establish the correct Mach number in the mixing tube and the desired ratio of weight flow through the ejector to weight flow being pumped. A limited study of wind-tunnel geometry indicated that it was desirable to use a supersonic diffuser and second minimum between the test section and the ejector. For the open test section the optimum contraction ratio for this diffuser appeared to be about 0.6. Tests of bluff bodies in open test sections indicated that the maximum-size body that could be tested would be considerably smaller than the size estimated on the basis of one-dimensional theory.

Langley Research Center,
National Aeronautics and Space Administration,
Langley Field, Va., April 16, 1959.

REFERENCES

1. Flügel, Gustav: The Design of Jet Pumps. NACA TM 982, 1941.

2. Johannesen, N. H.: Ejector Theory and Experiments. A. T. S. No. 1, Trans. Danish Acad. Tech. Sci. (Copenhagen), 1951.

3. Fox, N. L.: The Pumping Characteristics of Long Mixing Section Jet Pumps. Rep. No. SM-14385, Douglas Aircraft Co., Inc., May 7, 1952. (Rev. Sept. 5, 1952.)

4. Fabri, J., and Paulon, J.: Theory and Experiments on Supersonic Air-to-Air Ejectors. NACA TM 1410, 1958.

5. Hunczak, Henry R., and Rousso, Morris D.: Starting and Operating Limits of Two Supersonic Wind Tunnels Utilizing Auxiliary Air Injection Downstream of the Test Section. NACA TN 3262, 1954.

6. Maslach, G. J., and Sherman, F. S.: Design and Testing of an Axisymmetric Hypersonic Nozzle For a Low Density Wind Tunnel. WADC Tech. Rep. 56-341, ASTIA Doc. No. AD 97198, U. S. Air Force, Aug. 1956.

7. Syvertson, Clarence A., and Savin, Raymond C.: The Design of Variable Mach Number Asymmetric Supersonic Nozzles by Two Procedures Employing Inclined and Curved Sonic Lines. NACA TN 2922, 1953.

8. McLellan, Charles H., and Williams, Thomas W.: Liquefaction of Air in the Langley 11-Inch Hypersonic Tunnel. NACA TN 3302, 1954.

TABLE I

DESIGN COORDINATES FOR EJECTOR-NOZZLE CONTOUR

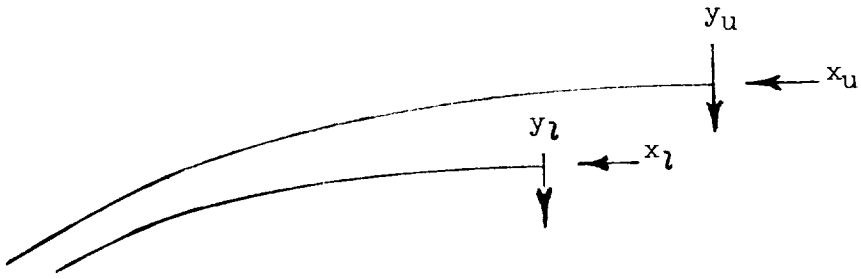

L-438

x_u	y_u	x_l	y_l
0	0	0	0
.1245	.0002	.1245	.0002
.2697	.0020	.2697	.0022
.4150	.0067	.4150	.0081
.5602	.0159	.5602	.0203
.7055	.0309	.7055	.0412
.8507	.0521	.8507	.0732
.9960	.0797	.9960	.1177
1.1412	.1138	1.1412	.1761
1.2865	.1548	1.2865	.2496
1.4317	.2066		
1.5770	.2698		
1.7222	.3412		
1.8675	.4214		

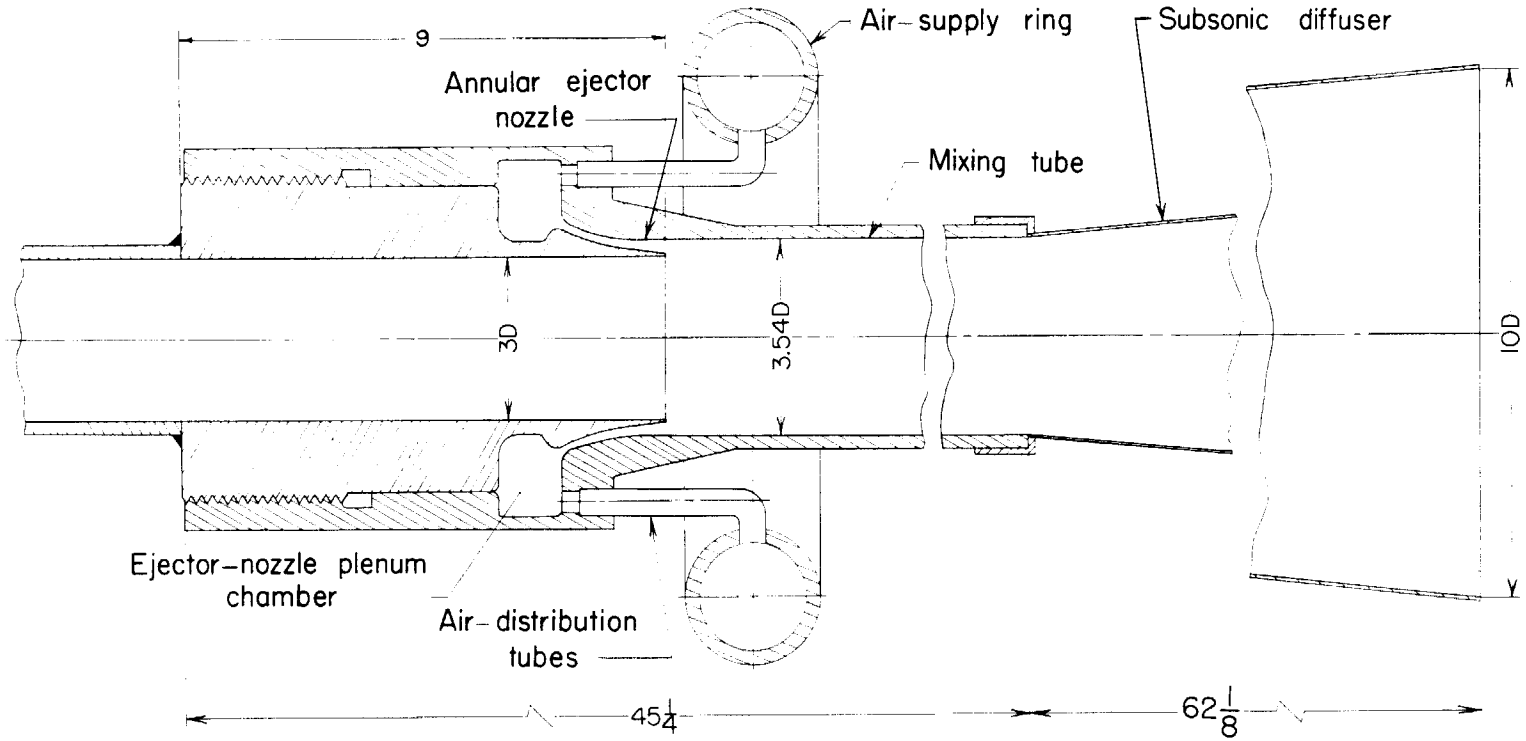

Figure 1.- Detailed sketch showing cross section of ejector 1. All dimensions are in inches.

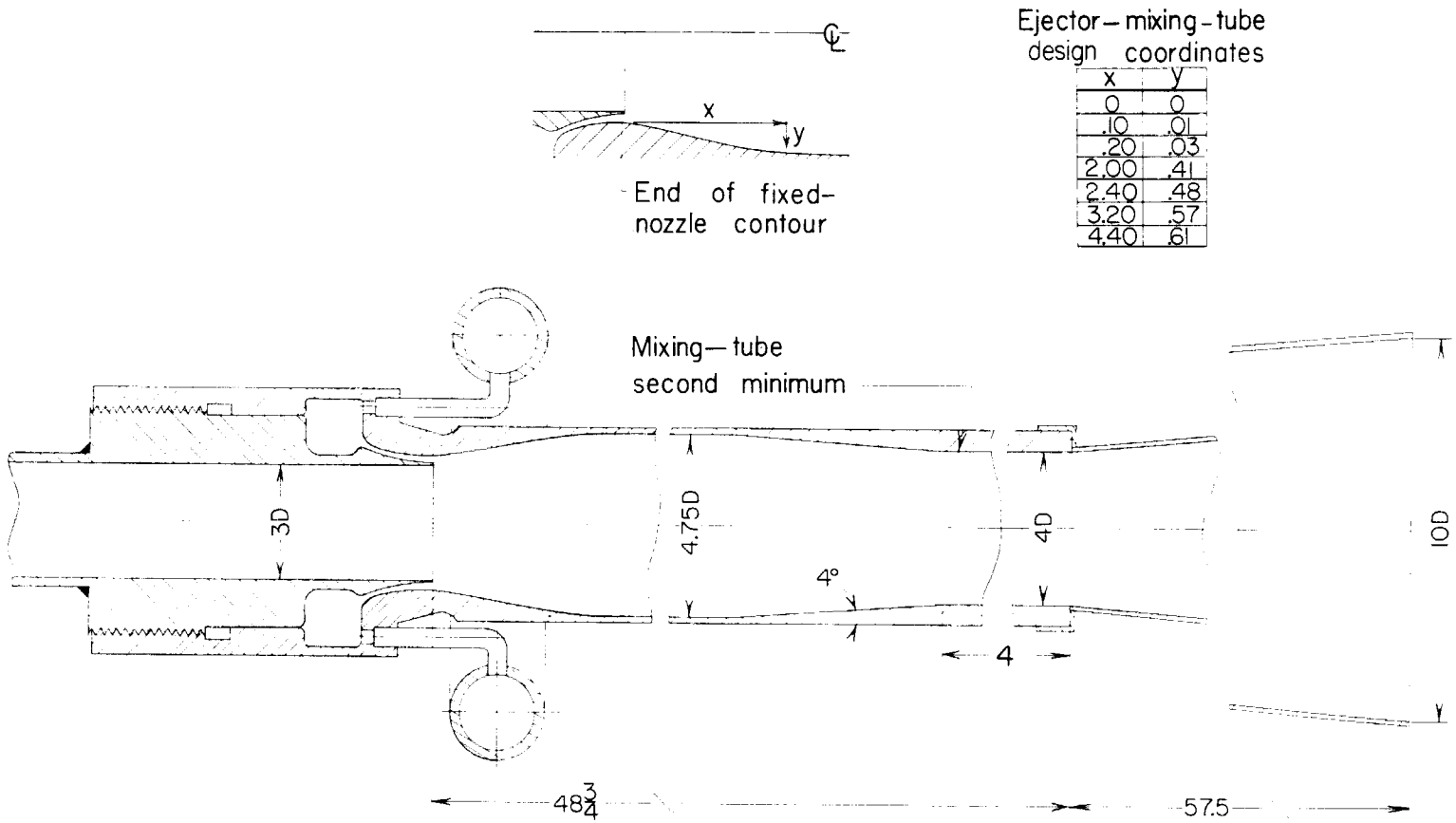

Figure 2.- Detailed sketch showing cross section of ejector 2. All dimensions are in inches.

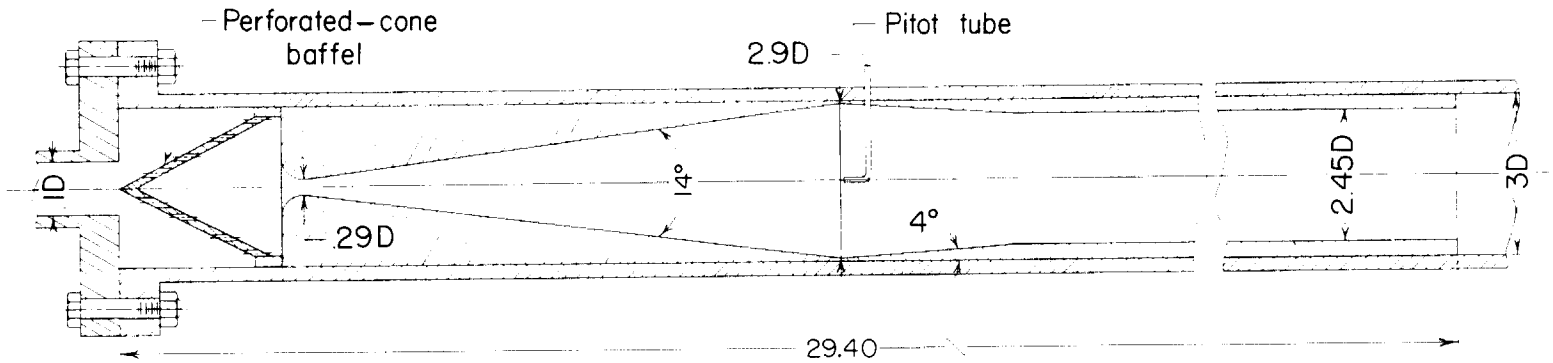

Figure 3.- Detailed sketch showing cross section of closed test section. All dimensions are in inches.

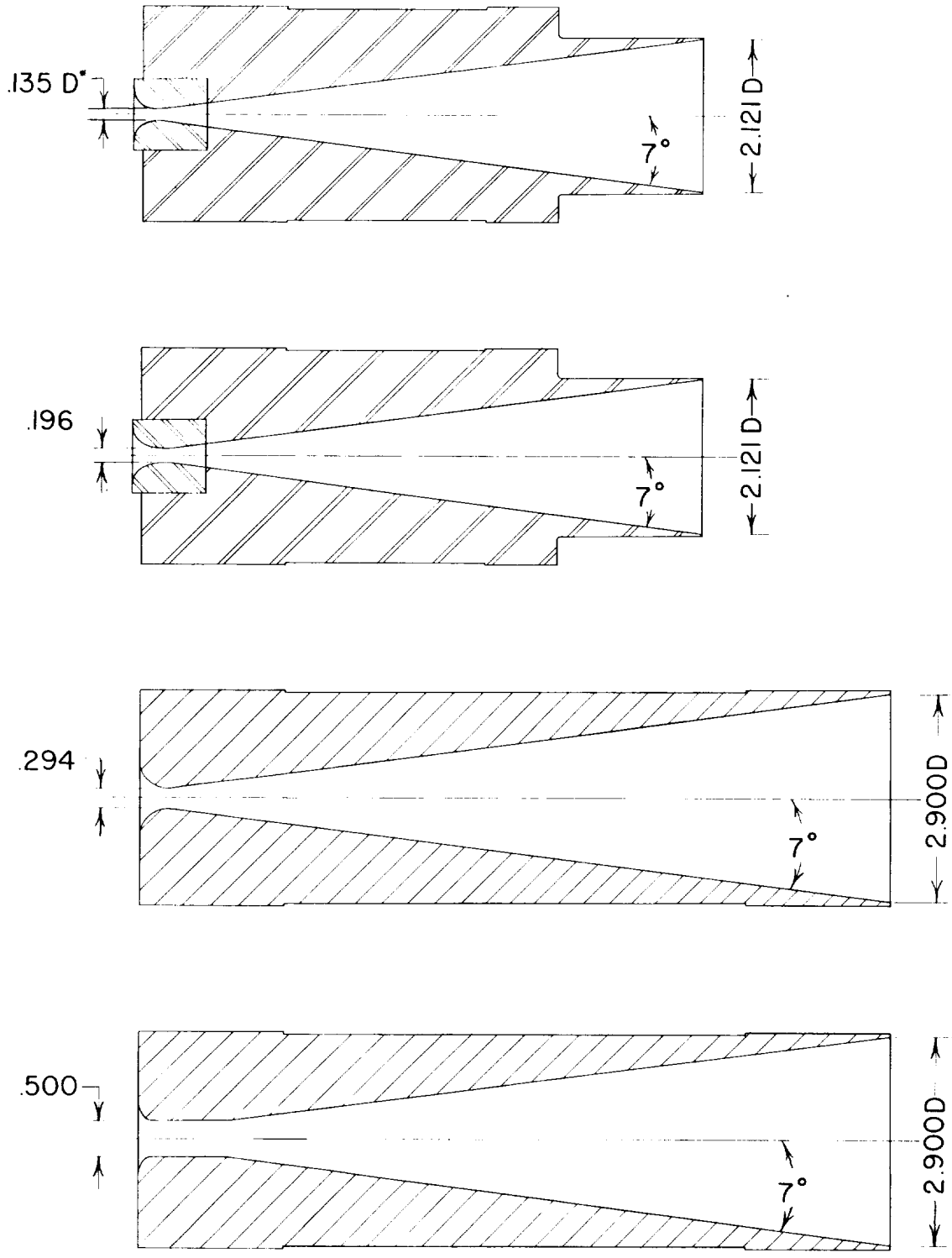

Figure 4.- Nozzles tested with open test section.

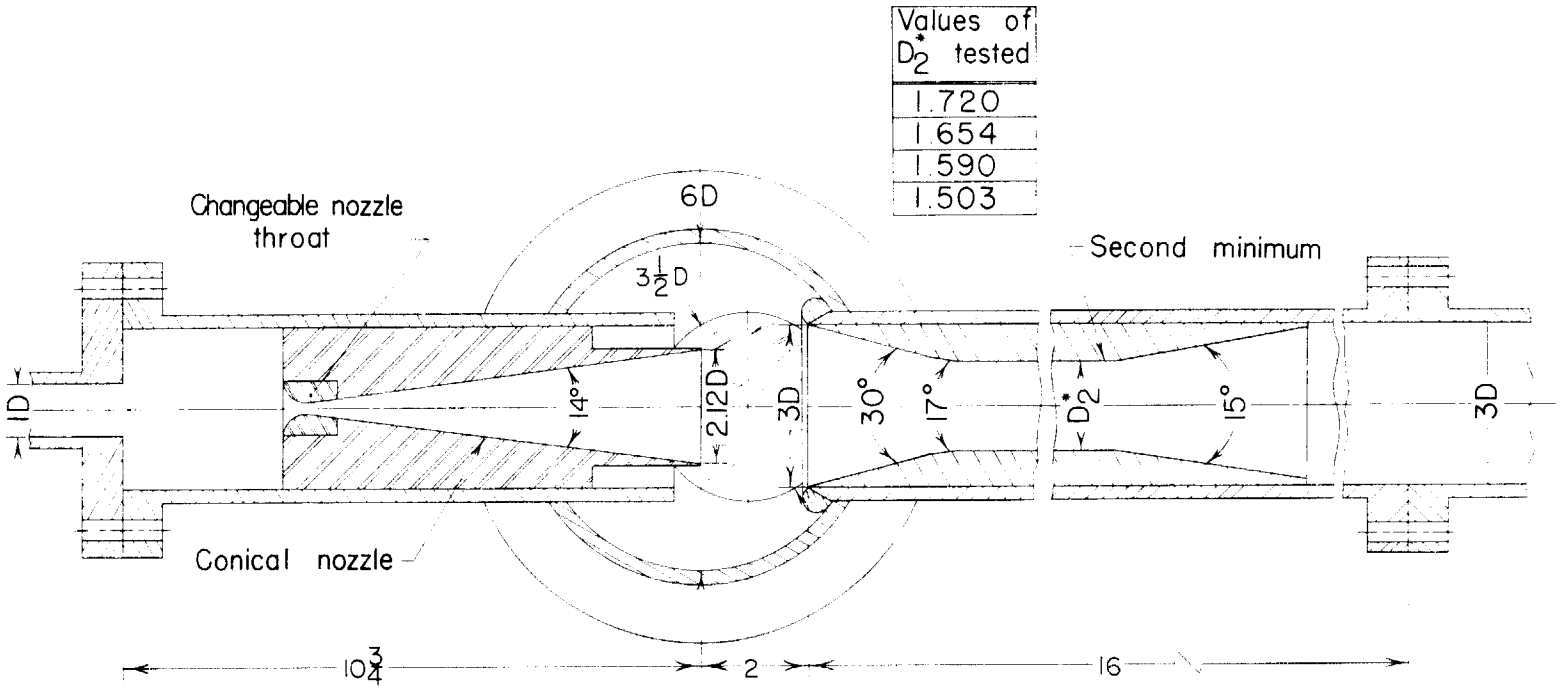

Figure 5.- Sketch showing details of open test section. All dimensions are in inches.

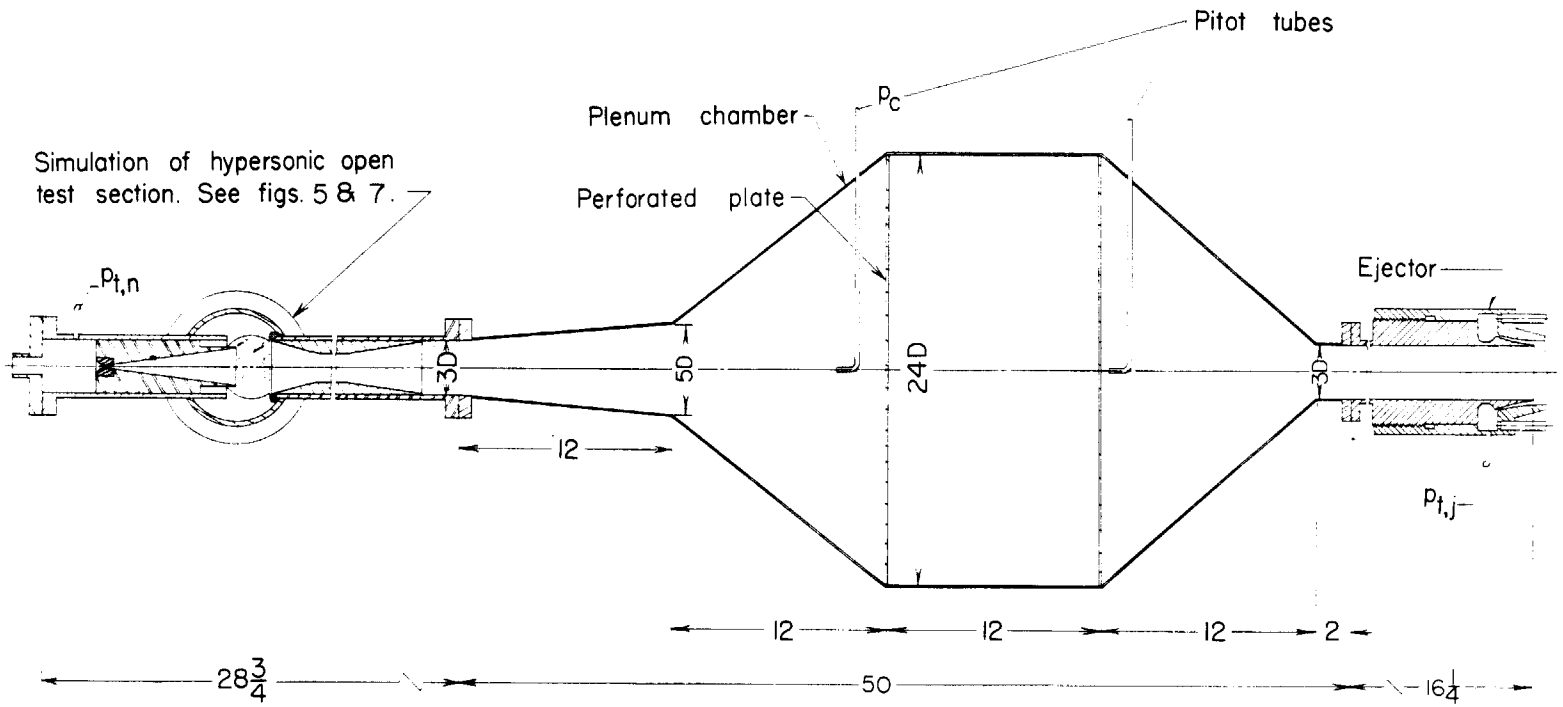

Figure 6.- Sketch showing overall arrangement of apparatus for determining ejector performance. All dimensions are in inches.

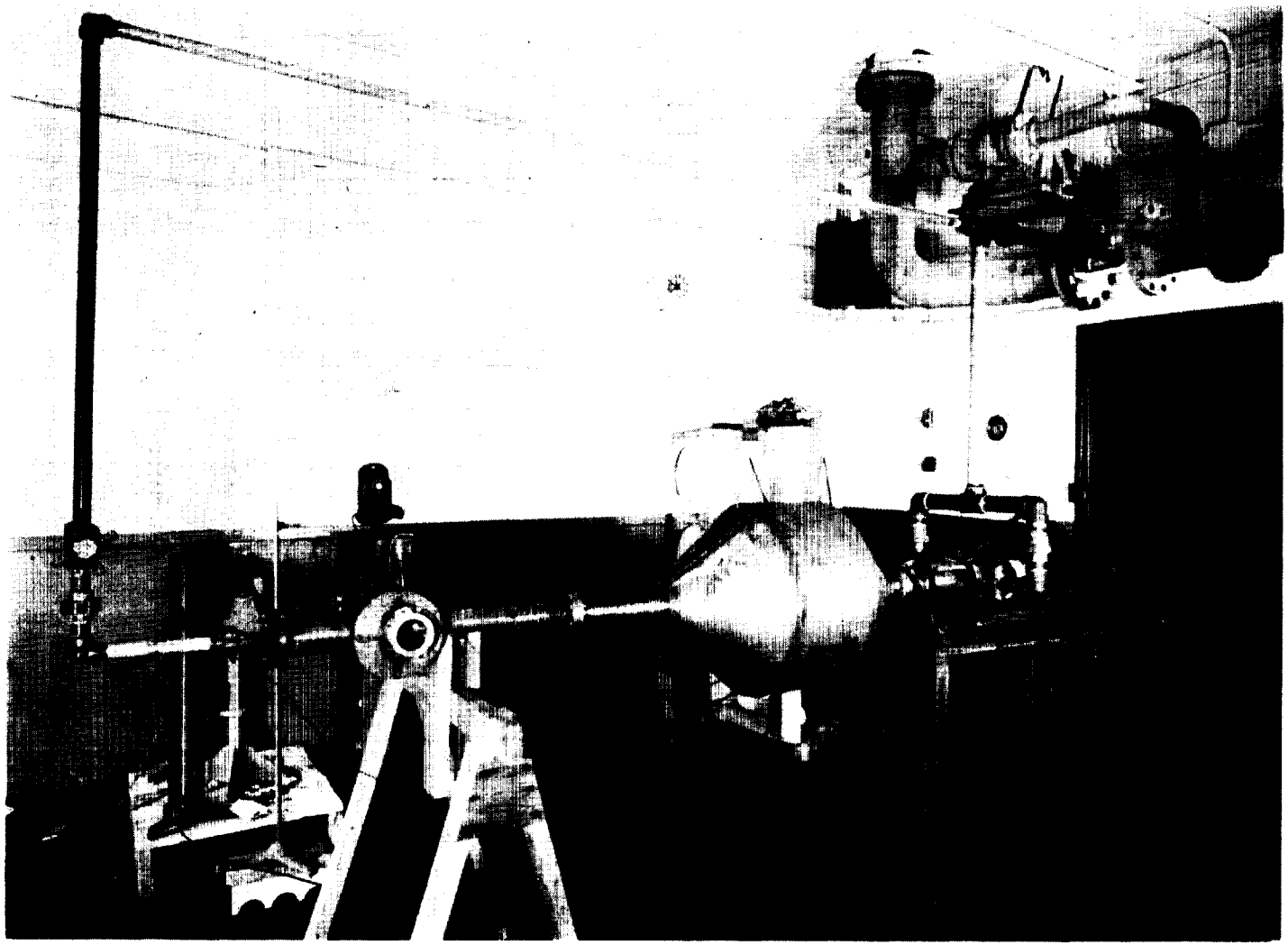

Figure 7.- Photograph of apparatus showing arrangement of components. L-58-3687

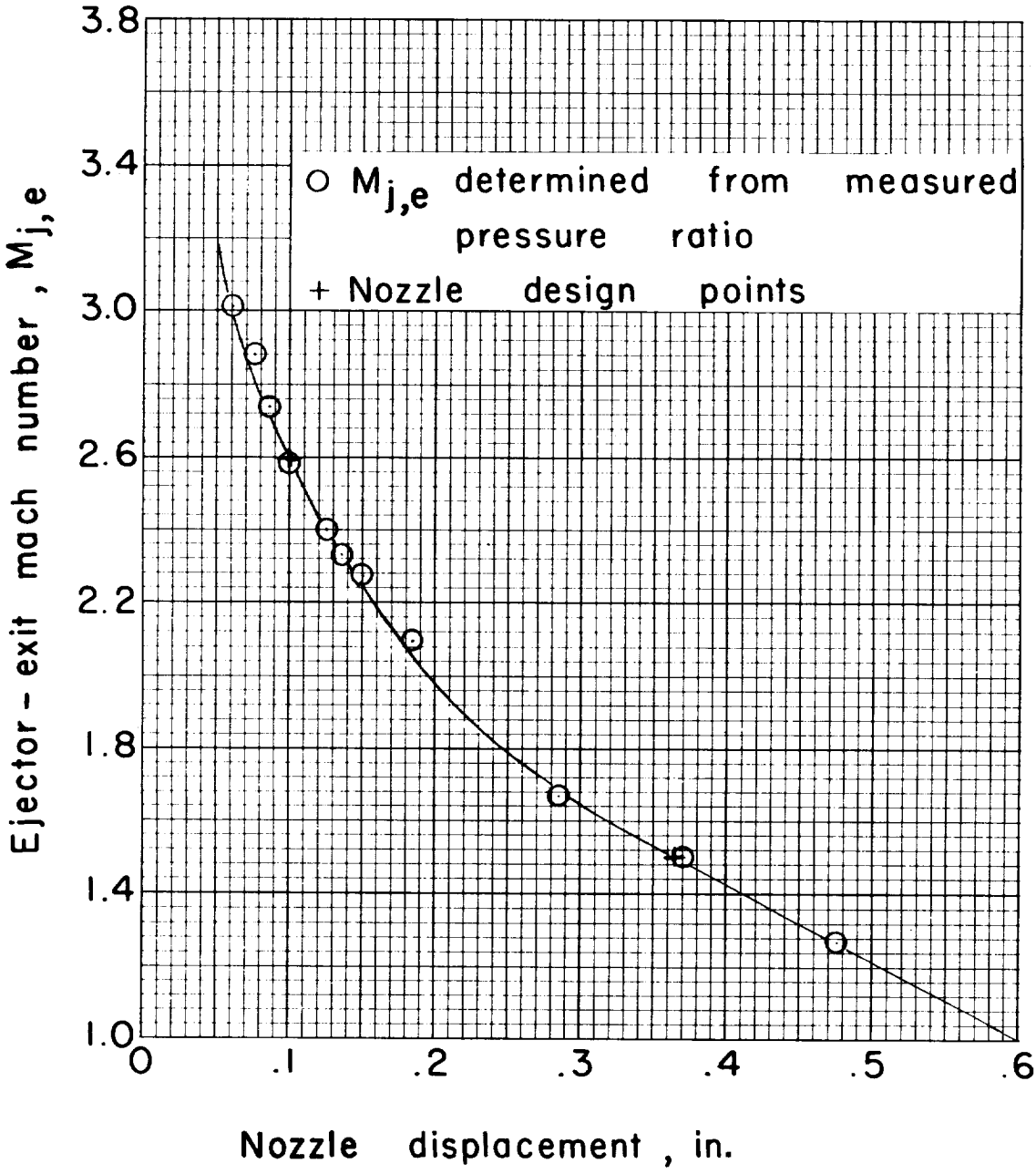

Figure 8.- Calibration of ejector-nozzle-exit Mach number with inner-nozzle-contour displacement (zero displacement corresponds to touching nozzle contours).

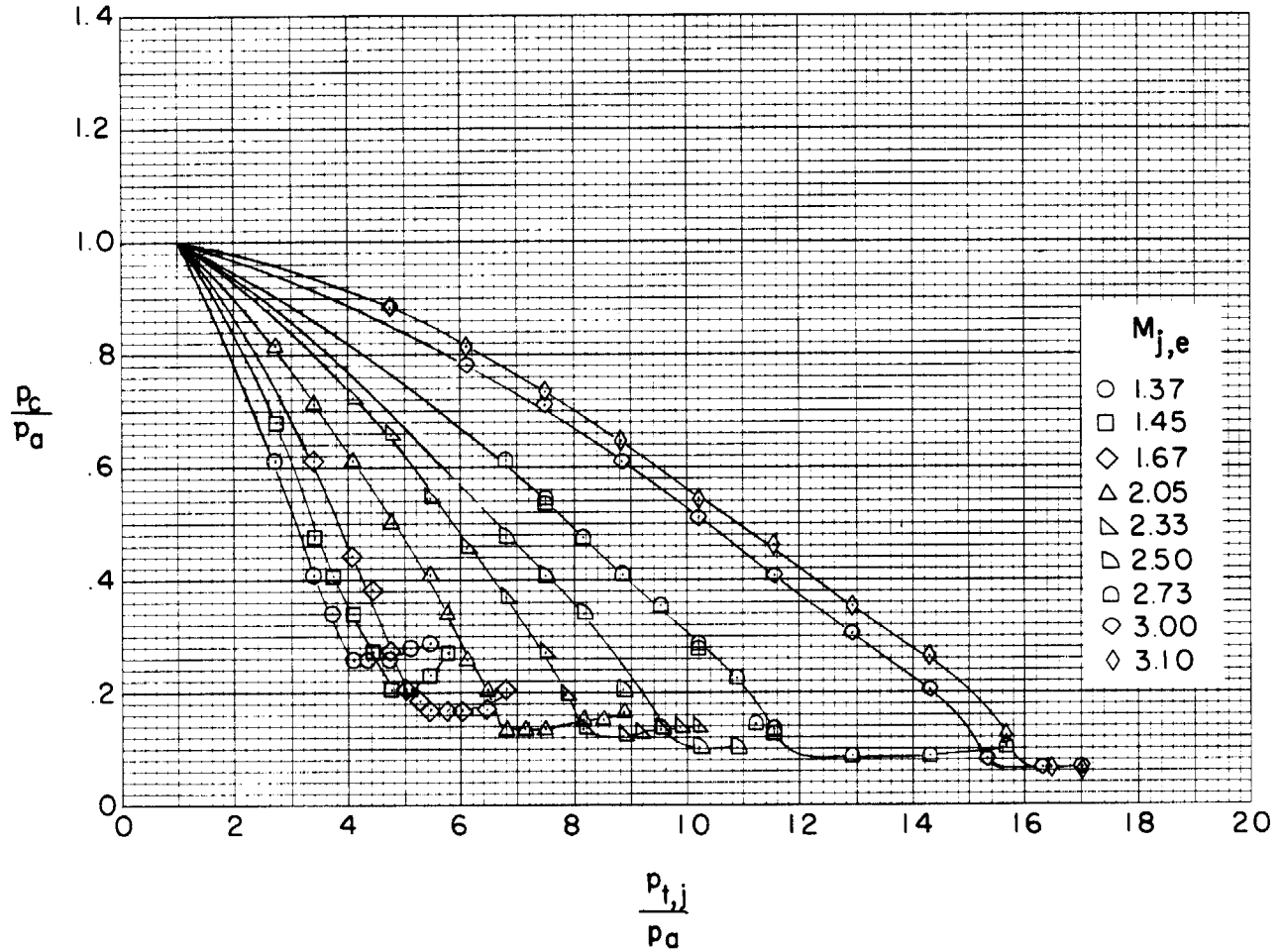

(a) Ejector 1.

Figure 9.- Variation of pressure to which ejector will pump as function of ejector stagnation pressure for various ejector-nozzle settings. No flow being pumped.

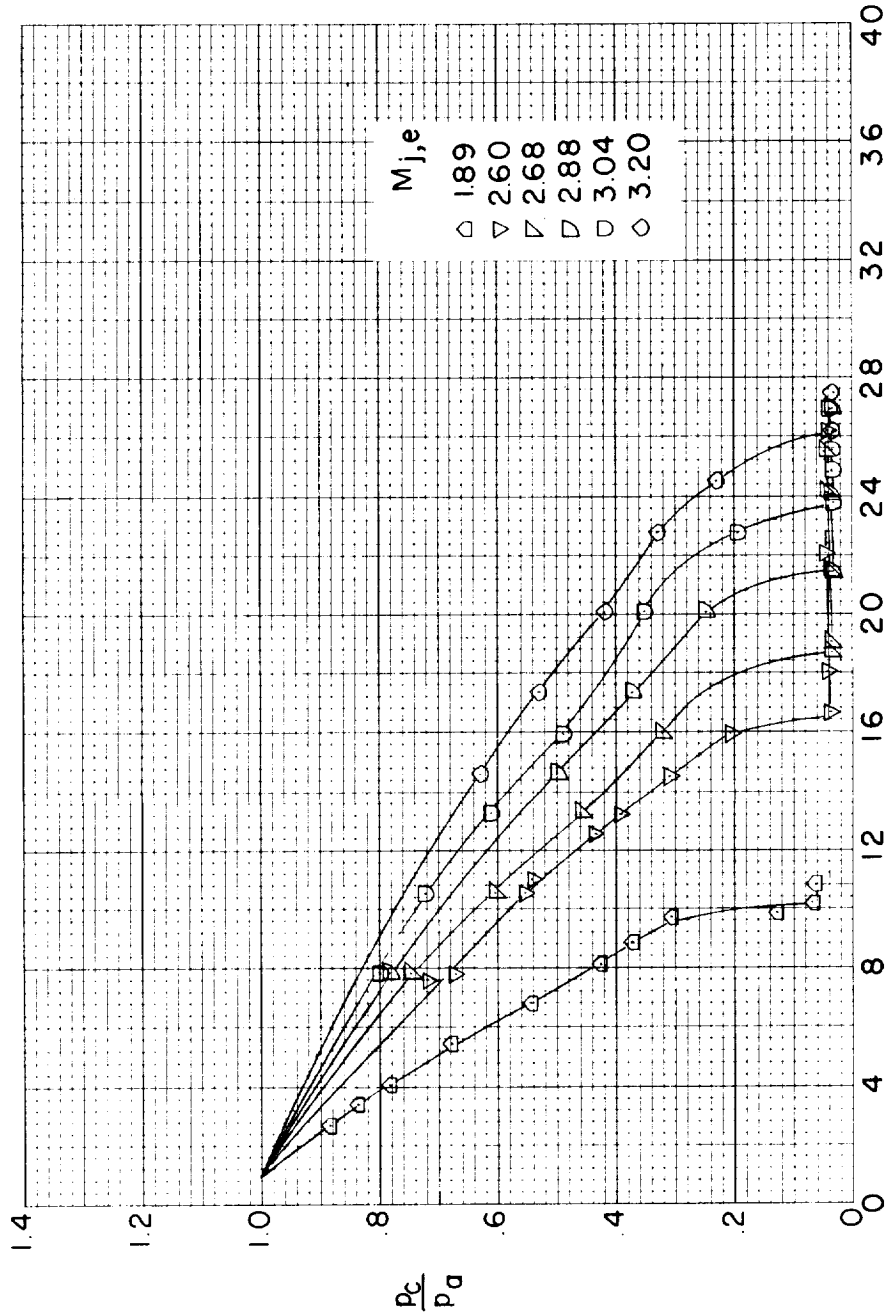

(b) Ejector 2.

Figure 9.- Concluded.

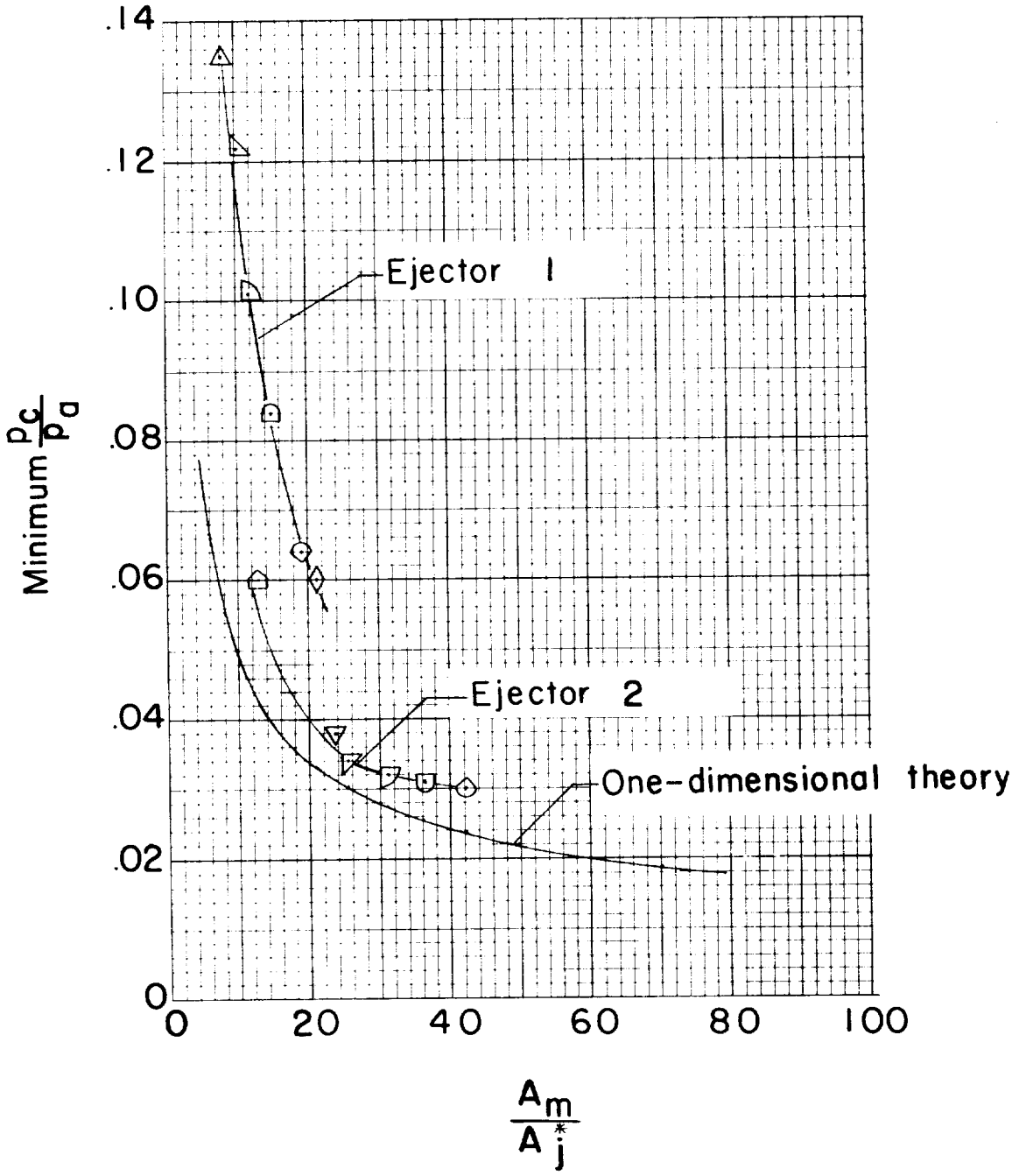

Figure 10.- Variation of minimum pressure to which ejector will pump as a function of the ratio of mixing-tube cross-sectional area to ejector-throat area. No flow being pumped.

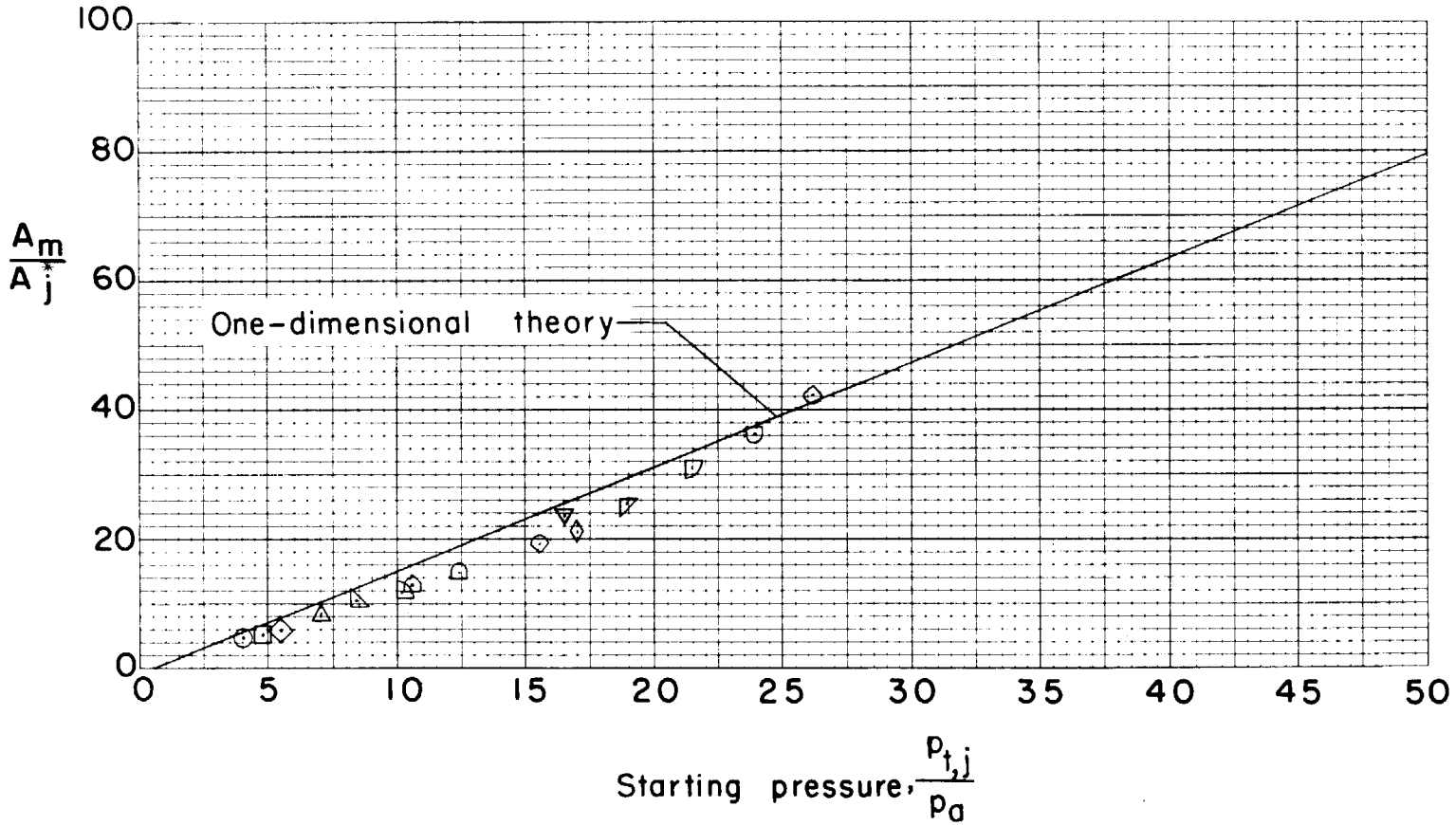

Figure 11.- Variation of pressure required to establish supersonic flow in mixing tube as function of ratio of cross-sectional area of mixing tube to minimum area of ejector nozzle. No flow being pumped.

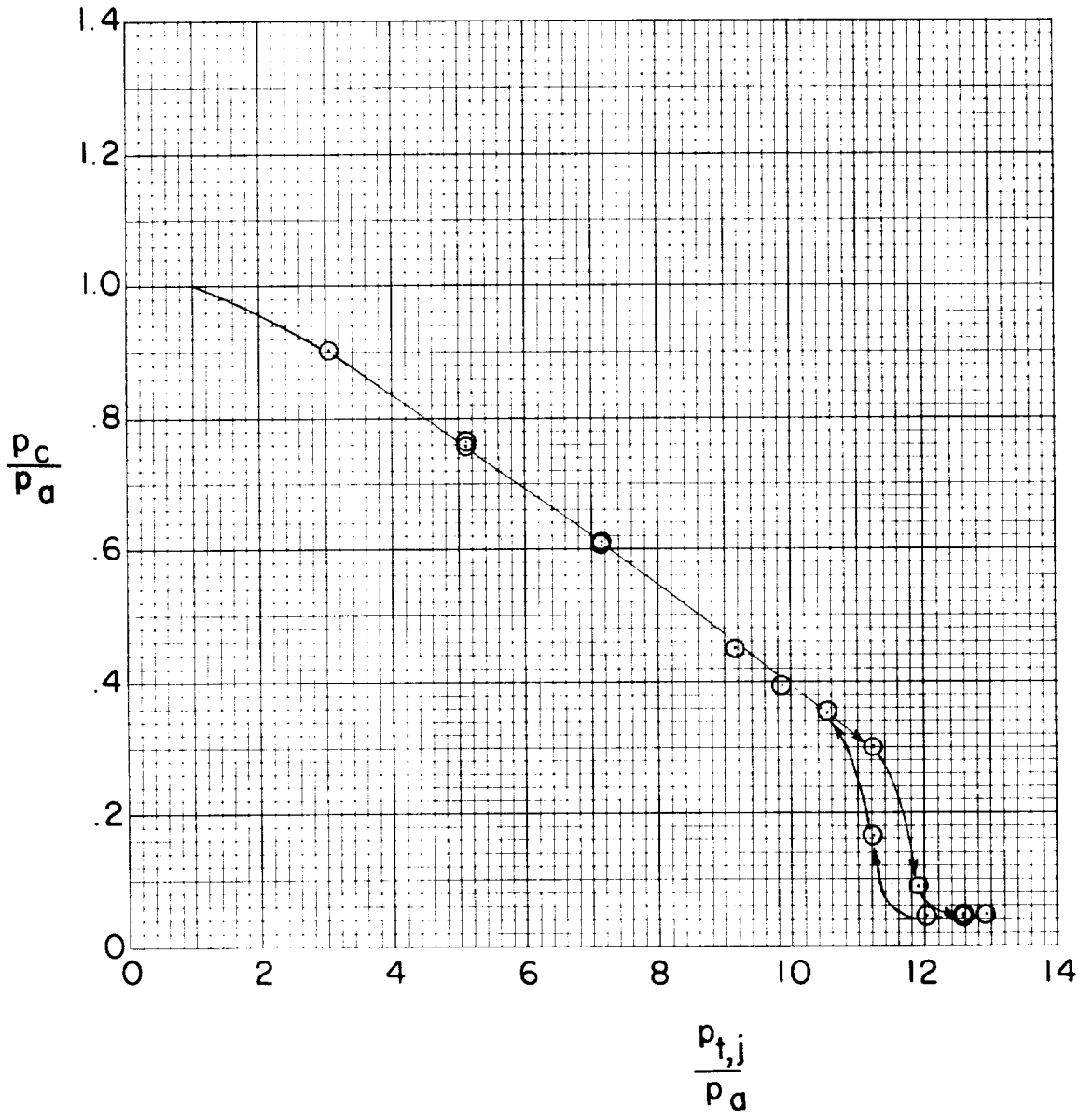

Figure 12.- Typical variation of pressure to which ejector will pump as a function of ejector stagnation pressure. Ejector 2; no flow being pumped; $M_{j,e} = 2.11$.

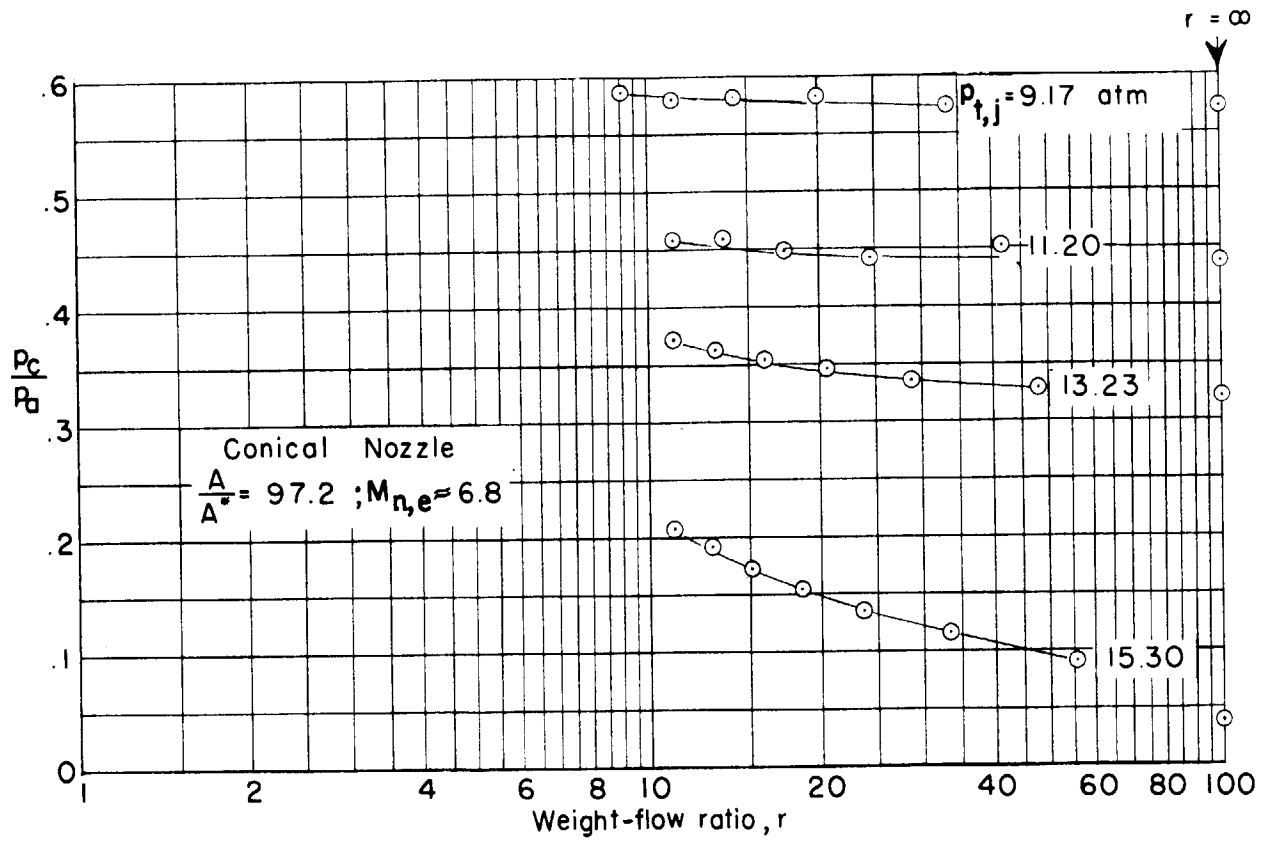

(a) $\frac{A_m}{A_j^*} = 23.65$.

Figure 13.- Variation of evacuation pressure produced by ejector 2 as function of weight-flow ratio r for various stagnation-pressure settings at three ejector-nozzle settings.

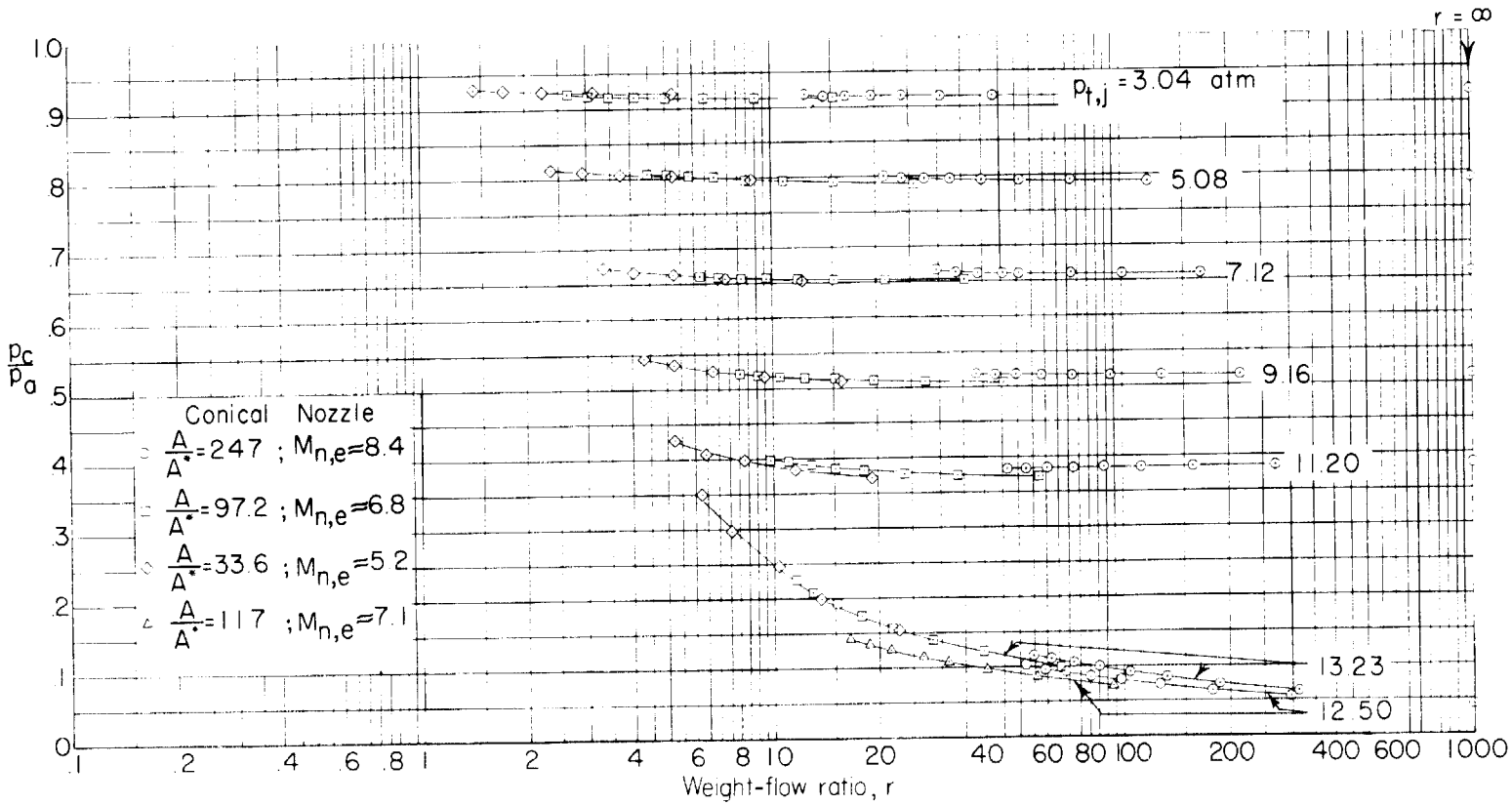

(b) $\frac{A_m}{A_j^*} = 17.21.$

Figure 13.- Continued.

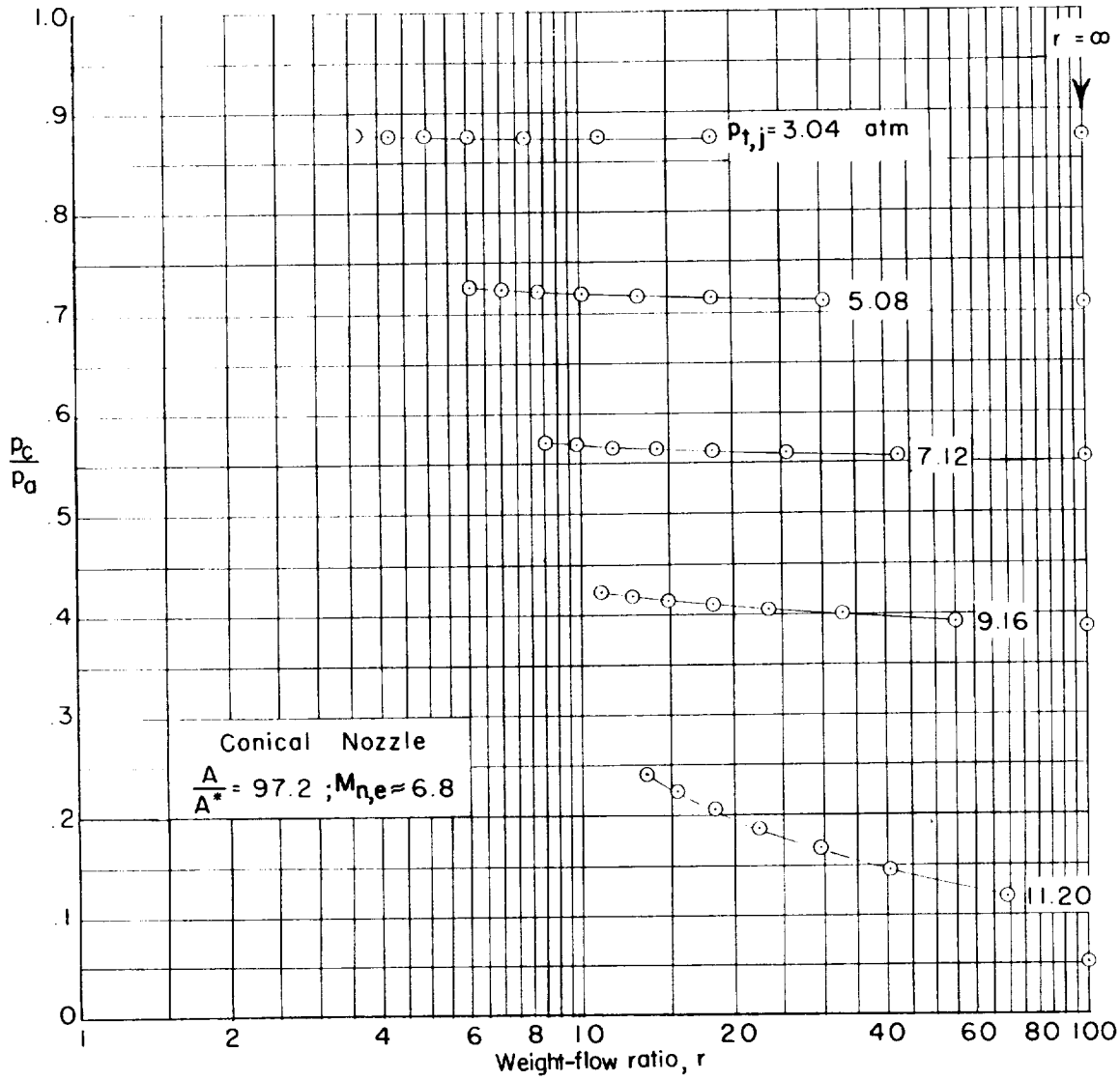

(c) $\frac{A_m}{A_j^*} = 14.31.$

Figure 13.- Concluded.

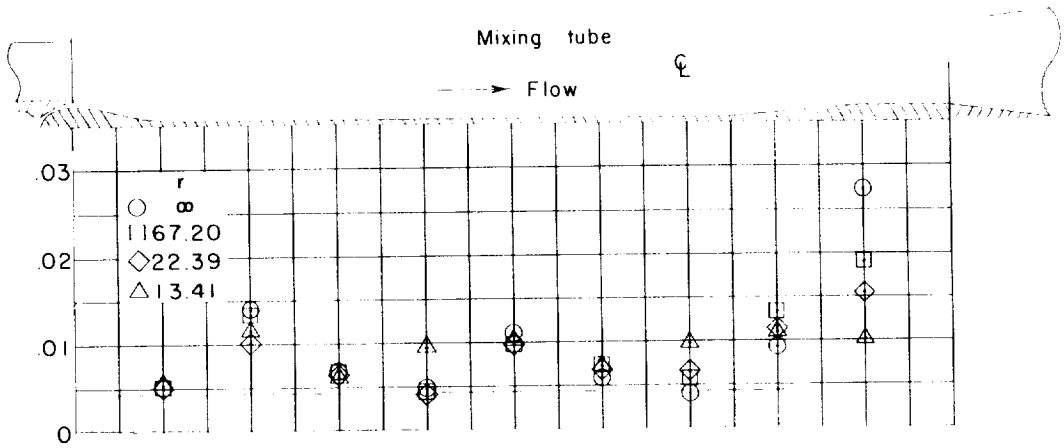

(a) $\frac{A_m}{A_j^*} = 14.31$; $p_{t,j} = 164.7$ psia.

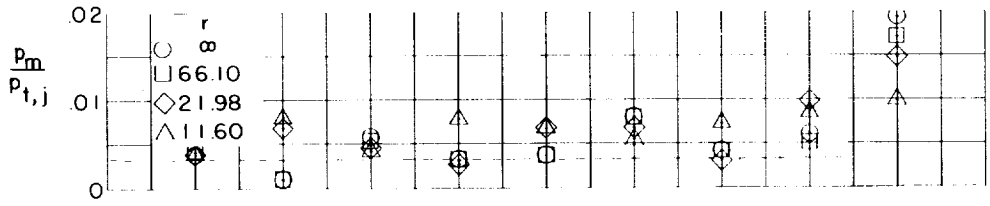

(b) $\frac{A_m}{A_j^*} = 17.21$; $p_{t,j} = 194.7$ psia.

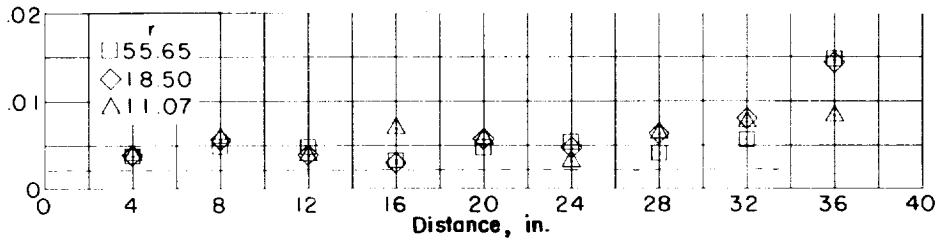

(c) $\frac{A_m}{A_j^*} = 23.65$; $p_{t,j} = 224.7$ psia.

Figure 14.- Typical pressure distribution in mixing tube for various ejector-exit Mach numbers and weight-flow ratios. Ejector 2; dashed lines indicate calculations by one-dimensional theory.

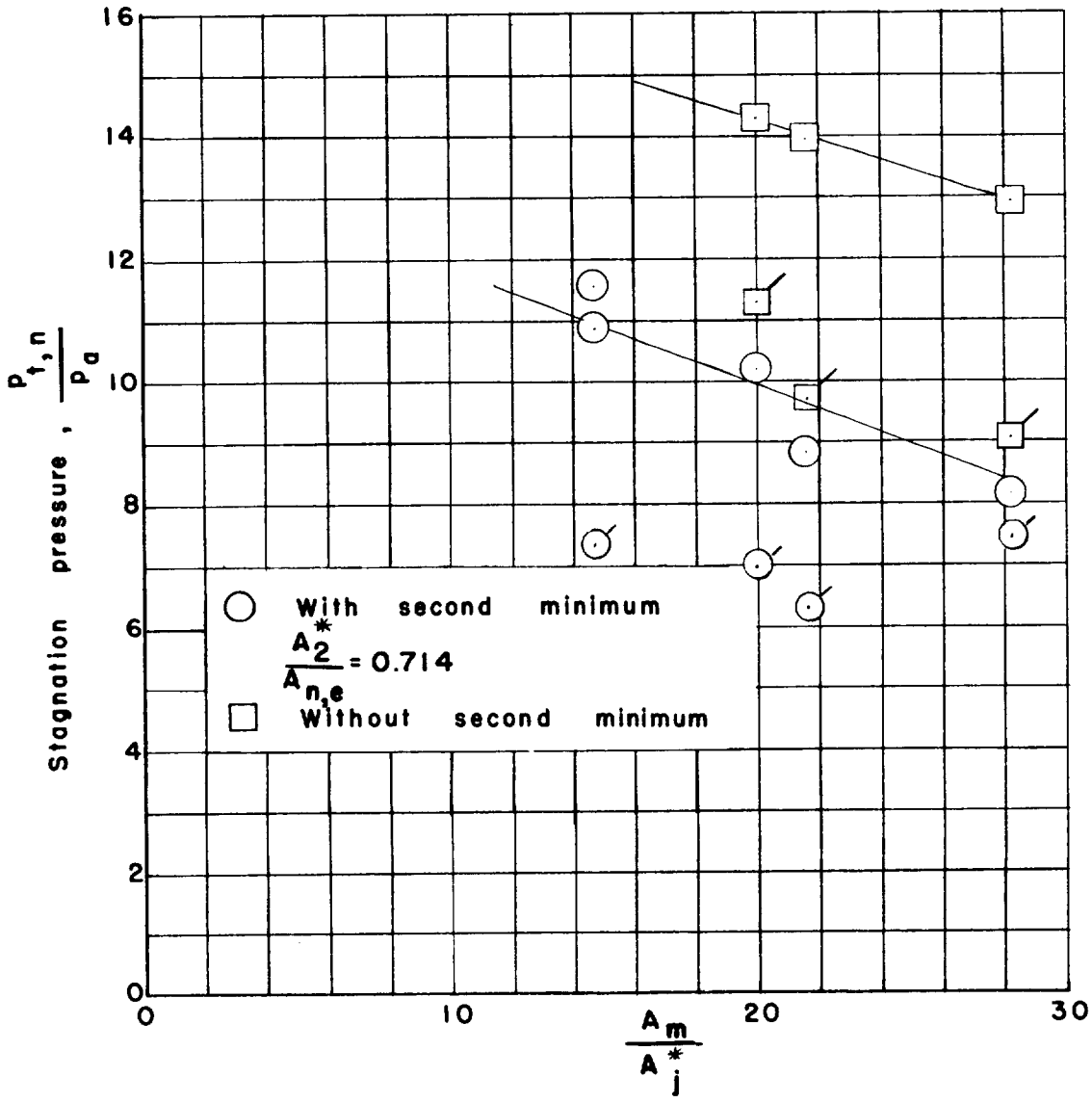

Figure 15.- Variation of nozzle stagnation pressure required for starting as a function of ejector-mixing-tube area ratio $\frac{A_m}{A^*_j}$. Ejector 1; $M_{n,e} \approx 6.8$; flagged symbols indicate calculated data from reference 5.

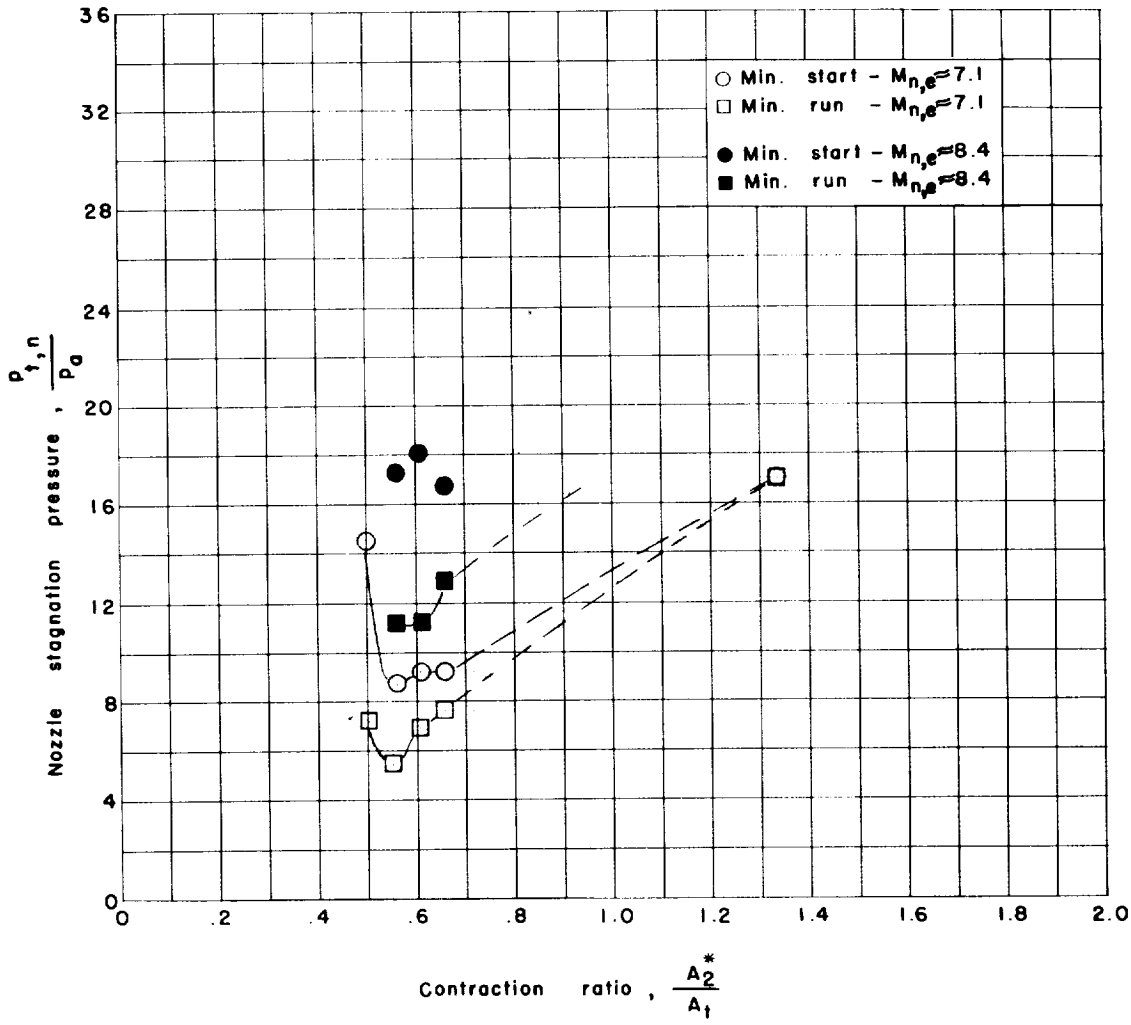

Figure 16.- Variation of the minimum starting and running pressures with second-minimum contraction ratio for $M_{n,e} \approx 7.1$ and $M_{n,e} \approx 8.4$ nozzles in open test section with ejector 2. $\frac{A_m}{A_j^*} = 16.5$; $P_{t,j} = 13.23$ atmospheres.

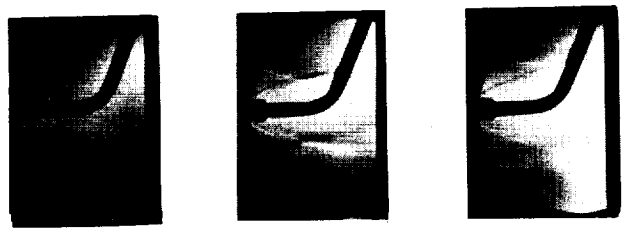

No flow $\frac{p_{t,n}}{p_a}=9.16$ $\frac{p_{t,n}}{p_a}=15.97$

(a) $\frac{D_b}{D_{n,e}} = 0.156.$

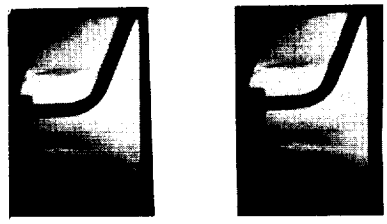

$\frac{p_{t,n}}{p_a}=11.20$ $\frac{p_{t,n}}{p_a}=15.28$

(b) $\frac{D_b}{D_{n,e}} = 0.214.$

$\frac{p_{t,n}}{p_a}=17.32$

(c) $\frac{D_b}{D_{n,e}} = 0.286.$

L-59-1942

Figure 17.- Schlieren pictures of flow about different-size bodies in open-test-section arrangement. Ejector 2; $\frac{p_{t,j}}{p_a} = 13.24$; $M_{n,e} \approx 7.1$.